



## DFT Studies on Structure-Property Relationship of $(I_2AlN_3)_n$ ( $n = 1-4$ ) Clusters

DENGXUE MA<sup>1</sup>, WENWEI ZHAO<sup>1</sup>, BAOHUI LI<sup>1</sup>, QIYING XIA<sup>1,2,\*</sup> and GUANGFU JI<sup>2,\*</sup>

<sup>1</sup>School of Chemistry and Chemical Engineering, Linyi University, Linyi 276005, P.R. China

<sup>2</sup>Laboratory for Shock Wave and Detonation Physics Research, Institute of Fluid Physics, Chinese Academy of Engineering Physics, Mianyang 621900, P.R. China

\*Corresponding authors: E-mail: xiaqiying@163.com, cyfjfk@caep.ac.cn

Received: 27 September 2013;

Accepted: 10 January 2014;

Published online: 16 September 2014;

AJC-15938

The clusters  $(I_2AlN_3)_n$  ( $n = 1-4$ ) were designed and investigated using density functional theory in order to find out the comprehensive relationships between structures and properties. The calculated results show that the Al-N<sub>α</sub> bonds form easily and Al-Al and N<sub>α</sub>-N<sub>α</sub> bonds are not found in the cyclic clusters  $(I_2AlN_3)_n$  ( $n = 2-4$ ). Trends in geometrical parameters with the oligomerization degree  $n$  are discussed. Frequency calculations are carried out on each optimized structure and IR spectra are discussed. Thermodynamic properties for the clusters  $(I_2AlN_3)_n$  ( $n = 1-4$ ) are linearly correlated with the oligomerization degree  $n$  as well as the temperature. Meanwhile, the dimerization, trimerization and tetramerization of the monomer  $I_2AlN_3$  are exothermic and favorable at temperatures up to 600 K.

**Keywords:**  $(I_2AlN_3)_n$  ( $n = 1-4$ ) clusters, Density functional theory (DFT), Structural feature, IR spectra, Thermodynamic properties.

### INTRODUCTION

Aluminum nitride (AlN) is widely used as microelectronics and optoelectronics due to excellent physical and chemical properties<sup>1</sup>. The common approach to AlN involves the reaction of trimethylaluminum (AlMe<sub>3</sub>) with ammonia (NH<sub>3</sub>) at a temperature in excess of 1050 °C<sup>2</sup>. However, high temperature may lead to unintentional nitrogen vacancies limiting the *p*-doping capability. Formation of composite nitrides with desired stoichiometric composition by chemical vapor deposition (CVD) method is a challenging task for chemists. To achieve this goal, single source precursors (SSP) which contain all necessary elements in desired stoichiometry ratio may be employed. Among these potential single source precursors, the ring compounds of group 13 metal azides attracted some attentions<sup>3-9</sup>. This is due to the azido group seems to be the optimal build-in nitrogen source and nitrides were successfully deposited without additional nitrogen sources.

The formed AlN has a high degree of carbon contamination due to pyrolysis of the organoaluminium azides<sup>3-5</sup>. McMurran *et al.*<sup>6-8</sup> reported several related routes for GaN synthesis utilizing a new class of inorganic azide compounds that incorporate hydrogen and halide ligands instead of organic groups. However, the inorganic metal azide clusters of aluminium have been the subject of few experimental studies<sup>9</sup>. So far, one never knows exactly how dangerous the target compounds and unwanted azide byproducts are, in other

words, it is still challenges to synthesize new azide precursors for a synthetic chemist. A good alternative to investigate the large variety of potential precursors is offered by theoretical computations.

In this paper, motivated by and based on previously studies on the clusters  $(H_2AlN_3)_n$  ( $n = 1-4$ )<sup>10</sup>,  $(F_2AlN_3)_n$  ( $n = 1-4$ )<sup>11</sup>, and  $(MYH_2)_4$  ( $M = B, Al, Ga; Y = N, P, As$ )<sup>12</sup>, we performed density functional theory (DFT) investigations the structural features, energies and IR spectra of  $(I_2AlN_3)_n$  ( $n = 1-4$ ) clusters, as well as the contributions of temperature and oligomerization degree  $n$  to the thermodynamic properties were established. The results are expected to provide further insight on the properties of group III A azide clusters, on one hand and also to shed some light into the trends with respect to cluster size. We hope that our theoretical predictions will stimulate further experimental efforts in the synthetic chemistry of novel group IIIA azide clusters.

### COMPUTATIONAL METHODS

All calculations were performed using the Gaussian 03 program<sup>13</sup> with the hybrid density-functional B3LYP method<sup>14</sup>. Moreover, the previous studies have shown that the B3LYP method is able to provide more reliable results<sup>10,11,15,16</sup>. Considering reasonable computational costs and accuracy, the 6-311 + G\* basis set for N and Al atoms<sup>17</sup>, and LanL2DZ basis set for I atoms were employed<sup>18</sup>. Harmonic vibrational analyses at the same level of theory were performed subsequently to

confirm that the located structures correspond to minima and to determine the zero-point vibrational energy corrections. A scaling factor of 0.96 was used to approximately correct the systematic overestimation of vibrational frequencies in the B3LYP calculation<sup>19</sup>.

## RESULTS AND DISCUSSION

**Geometrical structure and energy:** All of the optimized structures were characterized by the harmonic vibrational analyses to be true local energy minima on the potential energy surfaces without any imaginary frequency. The optimized geometries and symmetries of  $(I_2AlN_3)_n$  ( $n = 1-4$ ) clusters were presented in Fig. 1. Monomer  $I_2AlN_3$  was studied only as starting points for the oligomerizations. As can be seen from Fig. 1, monomer  $I_2AlN_3$  is a planar molecule of  $C_s$  symmetry (Fig. 1, 1A). Dimer  $(I_2AlN_3)_2$  is produced by the head-to tail dimerization of monomer  $I_2AlN_3$ . It contains a planar  $Al_2N_2$  core with  $D_{2h}$  symmetry (Fig. 1, 2A), which had been confirmed in the clusters  $(H_2AlN_3)_2$ <sup>10</sup> and  $(H_2GaN_3)_2$ <sup>6,7</sup>. Based on saturated organic six-membered rings existing in chair, boat, or twist-boat conformations, the similar conformations for trimer  $(I_2AlN_3)_3$  were considered and designed. However, only one twist-boat conformation with  $Al_3N_3$  six-membered ring (Fig. 1,

3A) was gained in the present study and the chair and boat conformations both have imaginary frequencies. The tetramers  $(I_2AlN_3)_4$  were produced by four  $I_2AlN_3$  oligomerizing *via* the  $\alpha$ -N atoms. They belong to  $C_1$  (4A),  $S_4$  (4B) and  $C_i$  (4C) symmetry, respectively, of which only the  $S_4$  symmetry structure with the  $N_3$  alternatively up and down has been suggested for the tetramers  $[(CH_3)ClAlN_3]_4$  and  $[(CH_3)BrAlN_3]_4$ <sup>5</sup> of the aluminium azides and the other two structures have not been found except that our group have reported<sup>10,11</sup>. As shown in Fig. 1,  $(I_2AlN_3)_n$  ( $n = 2-4$ ) clusters easily form Al-N $_{\alpha}$  adjoining ring structures, in which Al-Al and N $_{\alpha}$ -N $_{\alpha}$  bonds are not found.

For clarity, only the overall ranges of the optimized bond lengths and bond angles of  $(I_2AlN_3)_n$  ( $n = 1-4$ ) clusters at the DFT-B3LYP level were listed in Table-1. The bond lengths of N $_{\alpha}$ -N $_{\beta}$  and N $_{\beta}$ -N $_{\gamma}$  are in the range of 1.215-1.258 and 1.119-1.133 Å, respectively. The N $_{\alpha}$ -N $_{\beta}$  and N $_{\beta}$ -N $_{\gamma}$  bond lengths are very close to the N=N double bond (1.250 Å) and N=N triple bond (1.100 Å), respectively. As expected, two different bond lengths were found in the azide unit. The shorter bond length corresponds to the terminal N $_2$  (N $_{\beta}$ -N $_{\gamma}$ ) moiety, indicating a considerably activated azide towards N $_2$  elimination. As may be seen from Table-1, the average values of the Al-N $_{\alpha}$ , N $_{\alpha}$ -N $_{\beta}$  and Al-I bond lengths increase with the increase of the

TABLE -1  
RANGES OF THE BOND LENGTHS (Å), BOND ANGLES (°) AND ENERGIES (kJ mol<sup>-1</sup>)  
OF  $(I_2AlN_3)_n$  ( $n = 1-4$ ) CLUSTERS OPTIMIZED AT THE DFT-B3LYP LEVEL

	1A	2A	3A	4A	4B	4C
N $_{\beta}$ -N $_{\gamma}$	1.133	1.124	1.119- 1.121	1.120-1.121	1.119	1.121
N $_{\alpha}$ -N $_{\beta}$	1.215	1.235	1.248-1.255	1.252-1.258	1.255	1.253
Al-N $_{\alpha}$	1.781	1.954	1.961-1.975	1.969-1.994	1.958-1.982	1.975-1.984
Al-I	2.463-2.477	2.495	2.497-2.509	2.483-2.525	2.503-2.511	2.494-2.509
N $_{\alpha}$ -N $_{\beta}$ -N $_{\gamma}$	176.0	180.0	179.4-179.8	179.3-179.5	179.1	179.8-179.9
N $_{\beta}$ -N $_{\alpha}$ -Al	139.9	129.9	115.5-119.1	110.8-116.9	113.6-116.7	114.9-115.5
Al-N $_{\alpha}$ -Al		100.2	124.6-124.7	129.4-136.1	128.6	129.4-129.8
N $_{\alpha}$ -Al-N $_{\alpha}$		79.8	95.7-98.4	98.9-103.1	102.3	100.3-102.6
E	-1127975.77	-2256143.39	-3384216.05	-4512244.42	-4512279.90	-4512262.21
ZPE	40.34	85.93	129.85	172.21	173.31	172.75

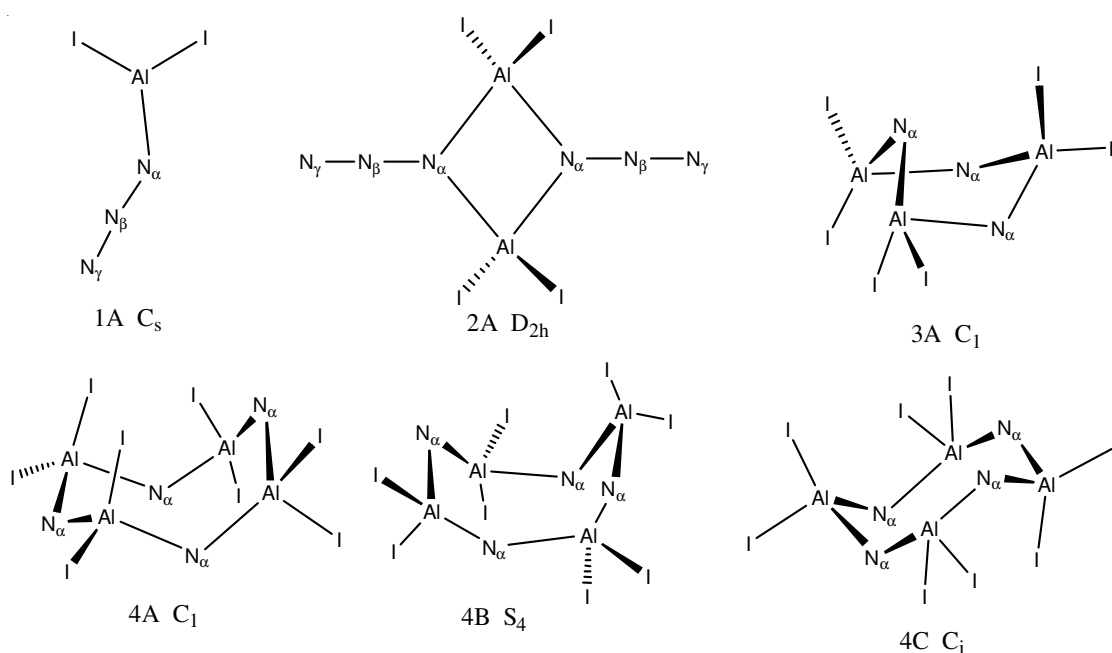


Fig. 1. Geometrical structures and symmetries of  $(I_2AlN_3)_n$  ( $n = 1-4$ ) clusters (N $_{\beta}$  and N $_{\gamma}$  atoms in trimers and tetramers are omitted for clarity)

oligomerization degree  $n$ . The average value of the  $N_\beta-N_\gamma$  bond lengths decreases from 1.133 Å in 1A to 1.119 Å in 4B and then tend to be constant at around 1.120 Å for trimer and tetramers. The  $N_\alpha-N_\beta$  and Al-I bond lengths outside of the rings increase as the cluster size is enlarged, which show it could easily eliminate  $N_2$  ( $N_\beta-N_\gamma$ ) and I groups to yield AlN material.

The azido group for monomer  $I_2AlN_3$  is slightly bent with  $N_\alpha-N_\beta-N_\gamma$  angles of  $176^\circ$  and those for  $(I_2AlN_3)_n$  ( $n = 2-4$ ) clusters are nearly linear with  $N_\alpha-N_\beta-N_\gamma$  angles in the range of  $179.1-180^\circ$ . Table-1 shows that  $N_\gamma$ ,  $N_\beta$ ,  $N_\alpha$  and Al atoms possess  $sp^2$ ,  $sp$ ,  $sp^2$  and  $sp^3$  hybridizations in the trimer and tetramer, respectively. The bond angles for  $N_\alpha-Al-N_\alpha$  and Al- $N_\alpha$ -Al increase as the cyclic clusters enlarge, while  $N_\beta-N_\alpha-Al$  bond angle decreases. The Al- $N_\alpha$ -Al bond angles in the cyclic clusters are consistently larger than  $N_\alpha-Al-N_\alpha$  bond angles. The smaller value for  $N_\alpha-Al-N_\alpha$  is in agreement with the larger size and the lower valence density around Al (due to its positive partial charge) and the consequently arising smaller repulsion between the bonding electron densities. Furthermore, as the oligomerization degree  $n$  increases, the trends of average geometrical parameters appear to be similar to those reported previously for  $(X_2AlN_3)_n$  ( $X = H, F; n = 1-4$ ) clusters<sup>10,11</sup>.

In order to obtain an appreciation for the thermodynamic stability of  $I_2AlN_3$  with respect to its oligomerization to  $(I_2AlN_3)_n$  ( $n = 2-4$ ) clusters, the values of the total energies ( $E$ ) and zero point energies (ZPE) for all the clusters are calculated at the DFT-B3LYP level and listed in Table-1. On the basis of energies of the tetramers listed in Table-1, the relative stability is in the following order:  $4B > 4C > 4A$ . Thus, the most stable isomers of  $(I_2AlN_3)_n$  ( $n=1-4$ ) clusters for each size are 1A, 2A, 3A and 4B.

**IR spectrum:** Fig. 2 presented the simulated IR spectra for the most stable geometric isomers of  $(I_2AlN_3)_n$  ( $n = 1-4$ ) clusters for each size based on the scaled harmonic vibrational frequencies obtained at the DFT-B3LYP level. Due to the complexity of vibrational modes, it is difficult to assign all bands. Therefore, only some typical vibrational modes are analyzed and discussed. It is evident from Fig. 2 that there are three strong characteristic regions: (1) One in the 2223-2197  $cm^{-1}$  region corresponds to the N-N asymmetric stretch of  $N_3$  groups and in this region, vibrations recorded equal those for  $N_3$  groups. For example, 3A has three bands at 2220, 2215, 2208  $cm^{-1}$ . (2) Another remarkable signal centering in 1386-1189  $cm^{-1}$  is associated with the N-N symmetric stretch of  $N_3$

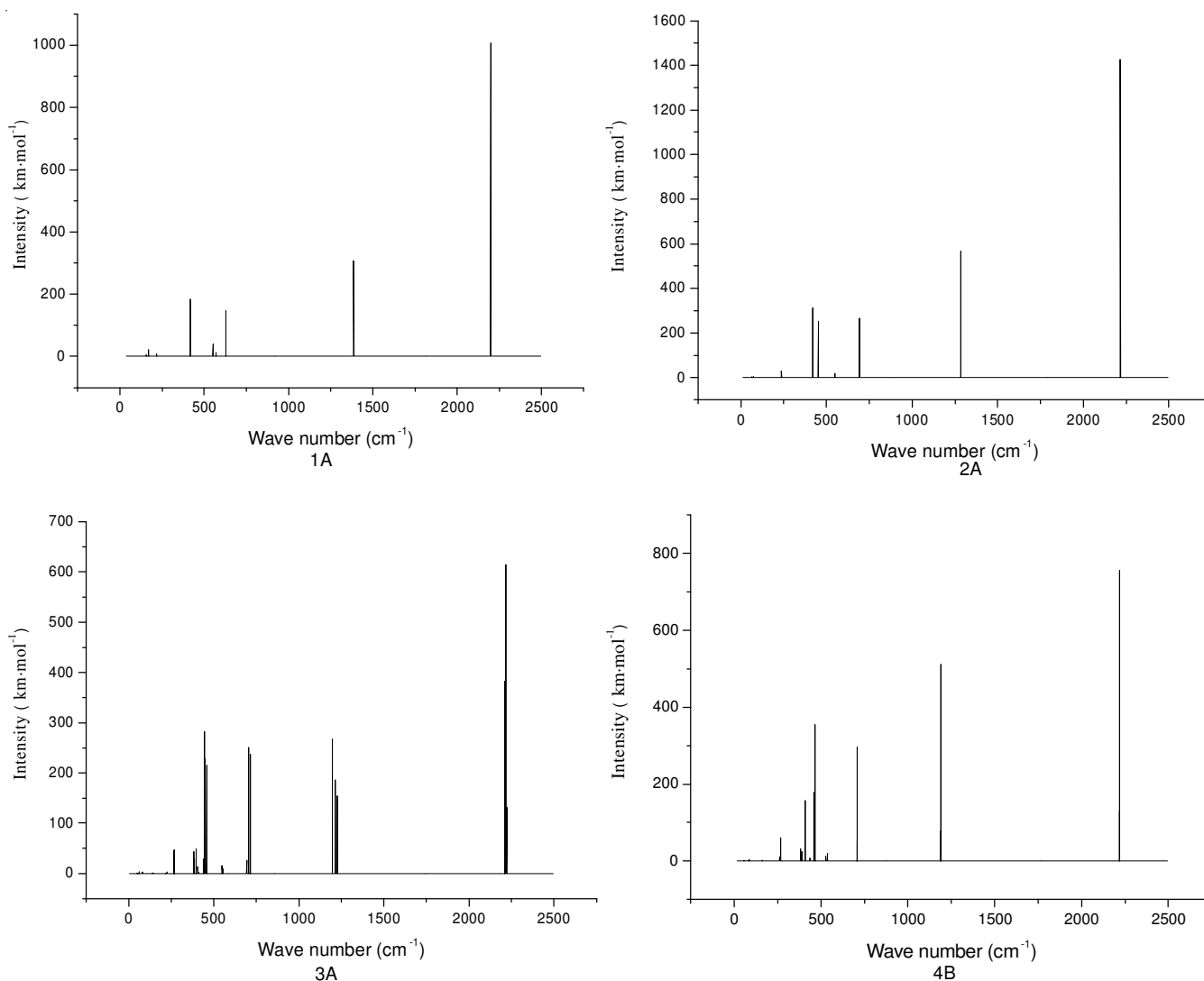


Fig. 2. IR spectra for the most stable isomers of  $(I_2AlN_3)_n$  ( $n = 1-4$ ) clusters

groups. And in agreement with the N-N asymmetric stretching vibrations, vibrations recorded also equal those for N<sub>3</sub> groups in this region. For example, 4B has four bands at 1198, 1193, 1191 and 1189 cm<sup>-1</sup>. In addition, its central position moves toward lower frequency as the cluster becomes larger. (3) The third region in the 716-5 cm<sup>-1</sup> is the fingerprint region, which can be used to identify and distinguish the isomeric configurations; and the peaks in this region are mainly caused by the stretching of rings, the asymmetric and symmetric stretching of Al-I, the wagging and scissoring of I-Al-I and the N<sub>3</sub> deformation vibrations.

**Thermodynamic properties:** Based on the above scaled vibrational results and statistical thermodynamic principle, the thermodynamic properties, such as standard molar heat capacity (C<sub>p,m</sub><sup>o</sup>), standard molar entropy (S<sub>m</sub><sup>o</sup>) and standard molar enthalpy (H<sub>m</sub><sup>o</sup>), ranging from 200 to 800 K for the most stable (I<sub>2</sub>AlN<sub>3</sub>)<sub>n</sub> (n = 1-4) clusters were obtained and listed in Table-2. It can be seen from Table-2 that all the thermodynamic quantities of (I<sub>2</sub>AlN<sub>3</sub>)<sub>n</sub> (n = 1-4) clusters increase with temperature evidently. This is because the main contributions to the thermodynamic functions are from the translations and rotations of molecules when temperature is low. However, at the higher temperature, the vibrational movement is intensified, which therefore makes more contributions to the thermodynamic properties, resulting in the increase in the thermodynamic functions. For intuitive illustration, taking monomer 1A as an example, the relationships between the thermodynamic functions and the temperature in the range 200-800 K were as follows,

$$C_{p,m}^o = 69.55144 + 0.12687 T - 7.89923 \times 10^{-5} T^2, \\ R^2 = 0.9929, SD = 1.0578$$

$$S_m^o = 293.76948 + 0.45844 T - 2.16722 \times 10^{-4} T^2, \\ R^2 = 0.9990, SD = 1.9282$$

$$H_m^o = -5.18416 + 0.0887 T + 2.26899 \times 10^{-5} T^2, \\ R^2 = 1.0000, SD = 0.1777$$

It is obvious that, when the temperature goes up, the increments decrease for both C<sub>p,m</sub><sup>o</sup> and S<sub>m</sub><sup>o</sup>, while increase for H<sub>m</sub><sup>o</sup> is constant. Since the coefficients of T<sup>2</sup> are very small, these correlations approximate to linear equations. In other words, thermodynamic functions of 1A increase linearly with the temperature on the whole.

In addition, all the thermodynamic functions for the most stable clusters (1A, 2A, 3A, 4B) increase with oligomerization degree n at the given temperature. The linear relationships between the thermodynamic functions and oligomerization degree n at 298.2 K can be described directly by the following equations:

$$C_{p,m}^o = -14.66 + 115.304 n$$

$$S_m^o = 215.73 + 207.913 n$$

$$H_m^o = -1.02 + 23.969 n$$

The correlation coefficients are all more than 0.99. On average, if one more I<sub>2</sub>AlN<sub>3</sub> is attached, C<sub>p,m</sub><sup>o</sup>, S<sub>m</sub><sup>o</sup> and H<sub>m</sub><sup>o</sup> increase by 115.30, 207.91 J mol<sup>-1</sup> K<sup>-1</sup> and 23.97 kJ mol<sup>-1</sup>, respectively, which shows good cluster additivity on the thermodynamic functions. The data of thermodynamic functions in Table-2 and the above analysis would be helpful for the further studies of the aluminum azides.

Table-3 summarized the entropy change (ΔS), enthalpy change (ΔH) and free energy change (ΔG) in the processes of 1A → 2A, 3A and 4B at temperatures in the range 200-800 K. All oligomerizations are disfavored by ΔS as shown in Table-3. The values of ΔH are negative at temperatures of 200-800 K, which denotes that these oligomerizations are exothermic. The values of ΔG for dimerizations are negative in the range of 200-800 K, However, the values of ΔG in the processes of 1A → 3A and 1A → 4B become positive as temperature increases up to 800 and 700 K, respectively. Which indicates those processes can occur spontaneously at temperatures up to 600 K. Therefore, these clusters (I<sub>2</sub>AlN<sub>3</sub>)<sub>n</sub> (n = 2-4) are stable under normal conditions. Moreover, the values of ΔH and ΔG increase from 200 to 800 K, which shows the binding forces of the clusters are weakened as the temperature increases.

## Conclusion

In this work, the equilibrium geometries, vibrational properties and stability of the designed (I<sub>2</sub>AlN<sub>3</sub>)<sub>n</sub> (n = 1-4) clusters have been studied using DFT-B3LYP method. The optimized clusters (I<sub>2</sub>AlN<sub>3</sub>)<sub>n</sub> (n = 2-4) all possess cyclic structure containing Al-N<sub>α</sub>-Al linkages and azido in azides has linear structure. An analysis of geometrical parameters shows it could easily eliminate N<sub>2</sub> (N<sub>β</sub>-N<sub>γ</sub>) and I<sup>-</sup> groups to yield AlN material. IR spectra of (I<sub>2</sub>AlN<sub>3</sub>)<sub>n</sub> (n = 1-4) clusters focus on three regions

TABLE-2  
THERMODYNAMIC PROPERTIES FOR THE MOST STABLE ISOMERS OF  
(I<sub>2</sub>AlN<sub>3</sub>)<sub>n</sub> (n = 1-4) CLUSTERS FOR EACH SIZE AT DIFFERENT TEMPERATURE<sup>a</sup>

	T	200	298.2	300	400	500	600	700	800
1A	C <sub>p,m</sub> <sup>o</sup>	90.45	101.28	101.44	108.19	112.85	116.35	119.09	121.27
	S <sub>m</sub> <sup>o</sup>	374.45	412.77	413.40	443.57	468.24	489.13	507.28	523.33
	H <sub>m</sub> <sup>o</sup>	13.68	23.14	23.32	33.83	44.89	56.36	68.14	80.16
2A	C <sub>p,m</sub> <sup>o</sup>	188.97	215.31	215.67	231.18	241.44	248.89	254.58	259.05
	S <sub>m</sub> <sup>o</sup>	563.23	644.10	645.43	709.77	762.53	807.23	846.05	880.34
	H <sub>m</sub> <sup>o</sup>	26.78	46.74	47.14	69.55	93.21	117.74	142.93	168.62
3A	C <sub>p,m</sub> <sup>o</sup>	290.11	330.62	331.19	355.21	370.98	382.28	390.84	397.51
	S <sub>m</sub> <sup>o</sup>	722.84	847.00	849.05	947.88	1028.94	1097.63	1157.23	1209.87
	H <sub>m</sub> <sup>o</sup>	40.02	70.67	71.28	105.70	142.06	179.75	218.42	257.85
4B	C <sub>p,m</sub> <sup>o</sup>	393.02	447.19	447.95	479.93	500.86	515.82	527.12	535.93
	S <sub>m</sub> <sup>o</sup>	870.11	1038.18	1040.95	1174.55	1284.04	1376.74	1457.14	1528.13
	H <sub>m</sub> <sup>o</sup>	53.57	95.06	95.89	142.41	191.51	242.38	294.55	347.72

a. Units: T (K); C<sub>p,m</sub><sup>o</sup> (J mol<sup>-1</sup> K<sup>-1</sup>); S<sub>m</sub><sup>o</sup> (J mol<sup>-1</sup> K<sup>-1</sup>); H<sub>m</sub><sup>o</sup> (kJ mol<sup>-1</sup>)

TABLE-3  
OLIGOMERIZATION ENTROPIES, ENTHALPIES AND GIBBS FREE ENERGIES AT DIFFERENT TEMPERATURE<sup>a</sup>

Processes	T	200	298.2	300	400	500	600	700	800
1A $\rightarrow$ (1/2)2A	$\Delta S$	-92.84	-90.72	-90.69	-88.69	-86.98	-85.52	-84.26	-83.16
	$\Delta H$	-93.69	-93.17	-93.15	-92.46	-91.69	-90.89	-90.08	-89.25
	$\Delta G$	-75.13	-66.12	-65.95	-56.98	-48.20	-39.58	-31.10	-22.72
1A $\rightarrow$ (1/3)3A	$\Delta S$	-133.50	-130.44	-130.38	-127.61	-125.26	-123.25	-121.54	-120.04
	$\Delta H$	-93.76	-93.00	-92.98	-92.02	-90.96	-89.86	-88.75	-87.63
	$\Delta G$	-67.06	-54.11	-53.86	-40.97	-28.33	-15.91	-3.68	8.40
1A $\rightarrow$ (1/4)4B	$\Delta S$	-156.92	-153.23	-153.16	-149.93	-147.23	-144.95	-143.00	-141.30
	$\Delta H$	-91.62	-90.71	-90.68	-89.56	-88.34	-87.10	-85.83	-84.56
	$\Delta G$	-60.24	-45.02	-44.73	-29.59	-14.73	-0.13	14.26	28.48

a. Units: T (K),  $\Delta S$  ( $J mol^{-1} K^{-1}$ ),  $\Delta H$  ( $kJ mol^{-1}$ ),  $\Delta G$  ( $kJ mol^{-1}$ )

of 1189-1386, 716-5 and 2223-2197  $cm^{-1}$ . Both 1386-1189 and 2223-2197  $cm^{-1}$  regions are characteristic vibrational spectra of  $N_3$  groups. Thermodynamic properties increase quantitatively with the increasing temperature and oligomerization degree  $n$ . At the same time, transformations from monomer (1A) to clusters (2A, 3A and 4B) are spontaneously exothermic processes at low temperatures.

#### ACKNOWLEDGEMENTS

The authors gratefully thank the National Natural Science Foundation of China (No. 21203086), Shandong Provincial Natural Science Foundation (No. ZR2012BL09) and Shandong Provincial Key Laboratory of Water and Soil Conservation & Environmental Protection (No. STKF201009).

#### REFERENCES

1. T.W. Hashman and S.E. Pratsinis, *J. Am. Ceram. Soc.*, **75**, 920 (1992).
2. A. Saxler, P. Kung, C.J. Sun, E. Bigan and M. Razeghi, *Appl. Phys. Lett.*, **64**, 339 (1994).
3. D.C. Boyd, R.T. Haasch, D.R. Mantell, R.K. Schulze, J.F. Evans and W.L. Gladfelter, *Chem. Mater.*, **1**, 119 (1989).
4. R.K. Schulze, D.C. Boyd, J.F. Evans and W.L. Gladfelter, *J. Vac. Sci. Technol. A*, **8**, 2338 (1990).
5. J. Kouvetakis, J. McMurran, C. Steffek, T.L. Groy, J.L. Hubbard and L. Torrisson, *Main Group Met. Chem.*, **24**, 77 (2001).
6. J. McMurran, J. Kouvetakis and D.J. Smith, *Appl. Phys. Lett.*, **74**, 883 (1999).
7. J. McMurran, D. Dai, K. Balasubramanian, C. Steffek, J. Kouvetakis and J.L. Hubbard, *Inorg. Chem.*, **37**, 6638 (1998).
8. J. McMurran, M. Todd, J. Kouvetakis and D.J. Smith, *Appl. Phys. Lett.*, **69**, 203 (1996).
9. K. Dehnicke and N. Krüger, *Z. Anorg. Allg. Chem.*, **444**, 71 (1978).
10. Q.Y. Xia, H.M. Xiao, X.H. Ju and X.D. Gong, *J. Phys. Chem. A*, **108**, 2780 (2004).
11. Q.Y. Xia, D.X. Ma, Q.F. Lin and W.W. Zhao, *Struct. Chem.*, **23**, 545 (2012).
12. A.Y. Timoshkin and H.F. Schaefer III, *J. Phys. Chem. A*, **114**, 516 (2010).
13. M.J. Frisch, G.W. Trucks, H.B. Schlegel, G.E. Scuseria, M.A. Robb, J.R. Cheeseman, J.A. Montgomery, Jr., T. Vreven, K.N. Kudin, J.C. Burant, J.M. Millam, S.S. Iyengar, J. Tomasi, V. Barone, B. Mennucci, M. Cossi, G. Scalmani, N. Rega, G.A. Petersson, H. Nakatsuji, M. Hada, M. Ehara, K. Toyota, R. Fukuda, J. Hasegawa, M. Ishida, T. Nakajima, Y. Honda, O. Kitao, H. Nakai, M. Klene, X. Li, J.E. Knox, H.P. Hratchian, J.B. Cross, V. Bakken, C. Adamo, J. Jaramillo, R. Gomperts, R.E. Stratmann, O. Yazyev, A.J. Austin, R. Cammi, C. Pomelli, J.W. Ochterski, P.Y. Ayala, K. Morokuma, G.A. Voth, P. Salvador, J.J. Dannenberg, V.G. Zakrzewski, S. Dapprich, A.D. Daniels, M.C. Strain, O. Farkas, D.K. Malick, A.D. Rabuck, K. Raghavachari, J.B. Foresman, J.V. Ortiz, Q. Cui, A.G. Baboul, S. Clifford, J. Cioslowski, B.B. Stefanov, G. Liu, A. Liashenko, P. Piskorz, I. Komaromi, R.L. Martin, D.J. Fox, T. Keith, M.A. Al-Laham, C.Y. Peng, A. Nanayakkara, M. Challacombe, P.M.W. Gill, B. Johnson, W. Chen, M.W. Wong, C. Gonzalez and J.A. Pople, Gaussian, Inc., Wallingford CT, Gaussian, Inc.: Pittsburgh, PA (2004).
14. A.D. Becke, *J. Chem. Phys.*, **98**, 5648 (1993).
15. Q.Y. Xia, Q.F. Lin and W.W. Zhao, *J. Mol. Model.*, **18**, 905 (2012).
16. Q.Y. Xia, D.X. Ma, W.W. Zhao and H.M. Xiao, *Chin. J. Chem.*, **29**, 1817 (2011).
17. M.J. Frisch, J.A. Pople and J.S. Binkley, *J. Chem. Phys.*, **80**, 3265 (1984).
18. P.J. Hay and W.R. Wadt, *J. Chem. Phys.*, **82**, 270 (1985).
19. A.P. Scott and L. Radom, *J. Phys. Chem.*, **100**, 16502 (1996).